Received: 7 October 2024 | Accepted: 2 March 2025

DOI: 10.1097/HEP.0000000000001316

ORIGINAL ARTICLE

OPEN

Early screening, diagnosis and recurrence monitoring of hepatocellular carcinoma in patients with chronic hepatitis B based on serum N-glycomics analysis: A cohort study

Rui Su[1,2,3,4] | Xuemei Tao[1,5] | Lihua Yan[1,2,3] | Yonggang Liu[1,6] | Cuiying Chitty Chen[7] | Ping Li[1,8] | Jia Li[1,9] | Jing Miao[1,10] | Feng Liu[1,9] | Wentao Kuai[1,11] | Jiancun Hou[1,12] | Mei Liu[13] | Yuqiang Mi[1,2,3,8] | Liang Xu[1,2,3,11]

[1]Clinical School of the Second People' s Hospital, Tianjin Medical University, Tianjin, China

[2]Tianjin Institute of Hepatology, Tianjin Second People's Hospital, Tianjin, China

[3]Department of Hepatology, Tianjin Integrated Traditional Chinese and Western Medicine Institute of Infectious Diseases, Tianjin, China

[4]Department of Precision Instruments and Opto-Electronics Engineering, Tianjin University, Tianjin, China

[5]Laboratory of Infectious and Liver Diseases, Center of Infectious Diseases, West China Hospital of Sichuan University, Chengdu, China

[6]Department of Pathology, Tianjin Second People's Hospital, Tianjin, China

[7]Department of Research and Development, Sysdiagno (Nanjing) Biotech Co. Ltd, Nanjing, Jiangsu Province, China

[8]Department of Integrated Traditional Chinese and Western Medicine, Tianjin Second People's Hospital, Tianjin, China

[9]Department of Hepatology, Tianjin Second People's Hospital, Tianjin, China

[10]Department of Traditional Chinese Medicine, Tianjin Second People's Hospital, Tianjin, China

[11]Department of Hepatology & Oncology, Tianjin Second People's Hospital, Tianjin, China

[12]Department of Surgery, Tianjin Second People's Hospital, Tianjin, China

[13]Department of Oncology, Beijing You'an Hospital, Capital Medical University, Beijing, China

Correspondence
Liang Xu, Department of Hepatology, Tianjin Second People's Hospital, Tianjin Research Institute of Liver Diseases, No. 7, Sudi South Road, Nankai District, Tianjin 300192, China.
Email: xuyangliang2004@163.com

Abstract

Background and Aims: HCC poses a significant global health burden, with HBV being the predominant etiology in China. However, current diagnostic markers lack the requisite sensitivity and specificity. This study aims to develop and validate serum N-glycomics-based models for the diagnosis and prognosis of HCC in patients with chronic hepatitis B–related cirrhosis.

Abbreviations: AFP, alpha-fetoprotein; AUC, area under the curve; BCLC, Barcelona Clinic Liver Cancer; CHB, chronic hepatitis B; CI, confidence interval; CNLC, China Liver Cancer Staging; CT, computed tomography; DFS, disease-free survival; DSA-FACE, DNA sequencer-assisted fluorophore-assisted carbohydrate electrophoresis; DCA, decision curve analysis; GnT-IVa, N-acetylglucosaminyltransferase IVa; GnT-V, N-acetylglucosaminyltransferase V; HBV, hepatitis B virus; HCC, hepatocellular carcinoma; HCC-GRF, hepatocellular carcinoma glycomics random forest model; HCC-GSVM, hepatocellular carcinoma glycomics support vector machine model; ML, machine learning; MMP, matrix metalloproteinase; MRI, magnetic resonance imaging; NA2F, bigalacto core-α-1,6-fucosylated biantennary glycan; NA2FB, bigalacto core-α-1,6-fucosylated bisecting biantennary glycan; NA3, tri-antennary glycan; NA3Fb, branching α-1,3-fucosylated tri-antennary glycan; NGA2F, agalacto core-α-1,6-fucosylated biantennary glycan; NGA2FB, agalacto core-α-1,6-fucosylated bisecting biantennary glycan; NPV, negative predictive value; PNGaseF, peptide N-glycosidase-F; PPV, positive predictive value; prog-G, prognostic glycomics; PIVKA-II, protein induced by vitamin K absence or antagonist-II; RF, random forest; ROC, receiver operating characteristic; SVM, support vector machine; TACE, transarterial chemoembolization.

Rui Su, Xuemei Tao, and Lihua Yan contributed equally to this work.

Supplemental Digital Content is available for this article. Direct URL citations are provided in the HTML and PDF versions of this article on the journal's website, www.hepjournal.com.

Yuqiang Mi, Department of Hepatology, Tianjin Second People's Hospital, Tianjin Research Institute of Liver Diseases, No. 7, Sudi South Road, Nankai District, Tianjin 300192, China. Email: yuqiangmi68@163.com

Jiancun Hou, Department of Surgery, Tianjin Second People's Hospital, No. 7, Sudi South Road, Nankai District, Tianjin 300192, China. Email: houjiancun@163.com.

Mei Liu, Department of Oncology, Beijing You'an Hospital, Capital Medical University, No.8, West Toujiao, Right Anmenwai, Fengtai District, Beijing 100069 China. Email: liumei@ccmu.edu.cn.

Approach and Results: This study enrolled a total of 397 patients with chronic hepatitis B–related cirrhosis and HCC for clinical management. N-glycomics profiling was conducted on all participants, and clinical data were collected. First, machine learning-based models, Hepatocellular Carcinoma Glycomics Random Forest model and Hepatocellular Carcinoma Glycomics Support Vector Machine model, were established for early screening and diagnosis of HCC using N-glycomics. The AUC values in the validation set were 0.967 (95% CI: 0.930–1.000) and 0.908 (0.840–0.976) for Hepatocellular Carcinoma Glycomics Random Forest model and Hepatocellular Carcinoma Glycomics Support Vector Machine model, respectively, outperforming AFP (0.687 [0.575–0.765]) and Protein Induced by Vitamin K Absence or Antagonist-II (PIVKA-II) (0.665 [0.507–0.823]). It also showed superiority in subgroup analysis and external validation. Calibration and decision curve analysis also showed good predictive performance. Additionally, we developed a prognostic model, the prog-G model, based on N-glycans to monitor recurrence in patients with HCC after curative treatment. During the follow-up period, it was observed that this model correlated with the clinical condition of the patients and could identify all recurrent HCC cases (n = 12) prior to imaging findings, outperforming AFP (n = 7) and PIVKA-II (n = 9), while also detecting recurrent lesions earlier than imaging.
Conclusions: N-glycomics models can effectively predict the occurrence and recurrence of HCC to improving the efficiency of clinical decision-making and promoting the precision treatment of HCC.

Keywords: chronic hepatitis B, diagnostic model, hepatocellular carcinoma, machine learning, N-glycomics, prognostic model

INTRODUCTION

HCC is a significant global health problem. According to the GLOBOCAN 2022 database,[1] the incidence of newly diagnosed liver cancer ranks sixth globally and fourth in China among all malignancies. Furthermore, the mortality rate of HCC ranks third globally and second in China among all malignancies. Nearly half of all liver cancer cases occur in China.[2] Chronic HBV infection is the main initiating factor for HCC, with 33% of HCC cases worldwide caused by HBV infection; this proportion reaches up to 60% in Asian and African regions.[3,4] Patients with HCC have poor outcomes, mainly due to the low rate of early diagnosis and the high recurrence rate after treatment.[5,6]

Currently, traditional HCC screening and recurrence prediction methods rely mainly on abdominal ultrasound examination combined with serum markers such as alpha-fetoprotein (AFP) and abnormal prothrombin fragment (PIVKA-II).[7,8] However, the sensitivity and specificity of these methods are not very good, and new strategies are needed to improve the accuracy of the diagnosis of HCC.[9,10]

N-glycosylation represents one of the most prevalent forms of protein modification.[11–13] Aberrant N-glycan modifications are closely associated with the pathogenesis of diverse diseases, including processes such as malignant transformation and tumor progression.[14,15] N-glycosylation can markedly affect biological processes such as cell adhesion, proliferation, and signal transduction, all of which are closely related to hepatocarcinogenesis.[15–17] DNA sequencer-assisted fluorophore-assisted carbohydrate electrophoresis technology, developed by Callewaer et al,[18] enables the rapid, convenient, and efficient detection of serum N-glycans, thus providing robust technical support for the application of N-glycans in HCC research. Previous studies have shown that serum N-glycan markers are promising, noninvasive diagnostic tools for differentiating liver fibrosis, cirrhosis, and HCC.[19–21] However, no study has comprehensively investigated the role of N-glycomics in the early

screening, diagnosis, and recurrence monitoring of HCC.

Machine learning (ML) is an interdisciplinary field.[22] With the advancement of artificial intelligence technology, the utilization of ML in clinical model construction has become increasingly pervasive.[23–25] In this study, we aimed to develop N-glycomics-based diagnostic and prognostic models for patients with CHB-related HCC, providing an innovative approach for early detection and precision medicine. This approach could effectively alleviate the disease burden of HCC, enhance the overall prognosis of the HCC population, and contribute to secondary and tertiary prevention of HCC.

METHODS

Study population

The diagnostic cohort enrolled 226 inpatients diagnosed with CHB-related cirrhosis at Tianjin Second Hospital between February 2017 and December 2022, composed of 70 patients with HCC and 156 without.

Prognostic cohort 1 included a total of 136 patients diagnosed with CHB-related HCC who underwent curative treatment (hepatectomy or curative ablation) at Tianjin Second Hospital from February 2018 to February 2022.

Prognostic cohort 2 consisted of patients diagnosed with CHB-related HCC who underwent curative treatment (hepatectomy or curative ablation) at Tianjin Second Hospital between January 2022 and April 2023, all of whom were histopathology confirmed to have HCC after surgery.

External validation cohort enrolled 102 inpatients diagnosed with CHB-related cirrhosis at Beijing You'an Hospital between January 2018 and December 2022, which composed of 49 patients with HCC and 53 without.

This study was conducted in accordance with the Helsinki Declaration guidelines. All participants provided informed consent, and the study received approval from the Ethics Committee of Tianjin Second Hospital (Supplemental Figure S1, Supplemental Digital Content 1, http://links.lww.com/HEP/J756).

Glycomics analysis

Serum N-glycan detection was conducted following previously described methods.[19] Initially, 2 μL of serum was treated with peptide N-glycosidase-F (PNGaseF; New England Biolabs) to release the N-glycans. Subsequently, 8-aminonaphtalene-1,3,6-trisulphonic acid (APTS) (Invitrogen) was introduced to label-free N-glycan, and neuraminidase (New England Biolabs) was used to eliminate sialic acid. The processed samples were then measured using an ABI 3500 Genetic Analyzer (Applied Biosystems). Serum N-glycan profile data were analyzed via GeneMapper software version 4.1. Each sample yielded 9 specific serum N-glycan peaks (Supplementary Figure S2, Supplemental Digital Content 1, http://links.lww.com/HEP/J756), and the abundance of each peak was quantified by normalizing its height to the sum of the heights of all 9 peaks. This normalization approach effectively corrects for batch effects.

More on the methodology section is detailed in the Supplemental Materials, Supplemental Digital Content 1, http://links.lww.com/HEP/J756.

RESULTS

Study design and patient baseline characteristics

The overall workflow and detailed participant recruitment information for each analysis in this study are shown in Figure 1. A total of 397 patients with CHB-related cirrhosis and HCC were included, including 3 cohorts: diagnosis cohort, prognosis cohort 1, and prognosis cohort 2.

A total of 226 patients with CHB-related cirrhosis were enrolled in diagnosis cohort, including 70 with HCC and 156 without HCC ($p < 0.05$, Supplemental Table S1, Supplemental Digital Content 1, http://links.lww.com/HEP/J756).

The prognostic cohorts included prognostic cohort 1 and prognostic cohort 2. Prognostic cohort 1, which included 136 patients with early-stage CHB-related HCC who underwent ablation or curative surgery at our hospital, was used to establish a prognostic model for HCC. All patients had postoperative serum samples and follow-up data regarding recurrence. Serum samples were obtained after surgery without recurrence, and AFP and PIVKA-II data were concurrently collected at the corresponding time points. The follow-up duration for patients in prognostic cohort 1 was 20.73 (2.43–58.13) months, and the corresponding Disease-Free Survival (DFS) rates at 1, 2, and 3 years were 81.59%, 65.17%, and 55.47%, respectively. The median DFS was 38.1 (95% CI: 30.1-not reached) months, and 50 patients reached the DFS endpoint. The survival curve for prognostic cohort 1 is shown in Figure 2B. Prognostic cohort 2 was used for postoperative recurrence monitoring of patients with HCC and included 35 patients with CHB-related HCC who had received ablation or curative surgery. Serum samples, AFP levels, PIVKA-II levels, and imaging data at multiple time points for each patient were collected (Supplemental Table S2, Supplemental Digital Content 1, http://links.lww.com/HEP/J756), ranging from 4 to 14 cases (Figure 2A). The follow-up time for patients in

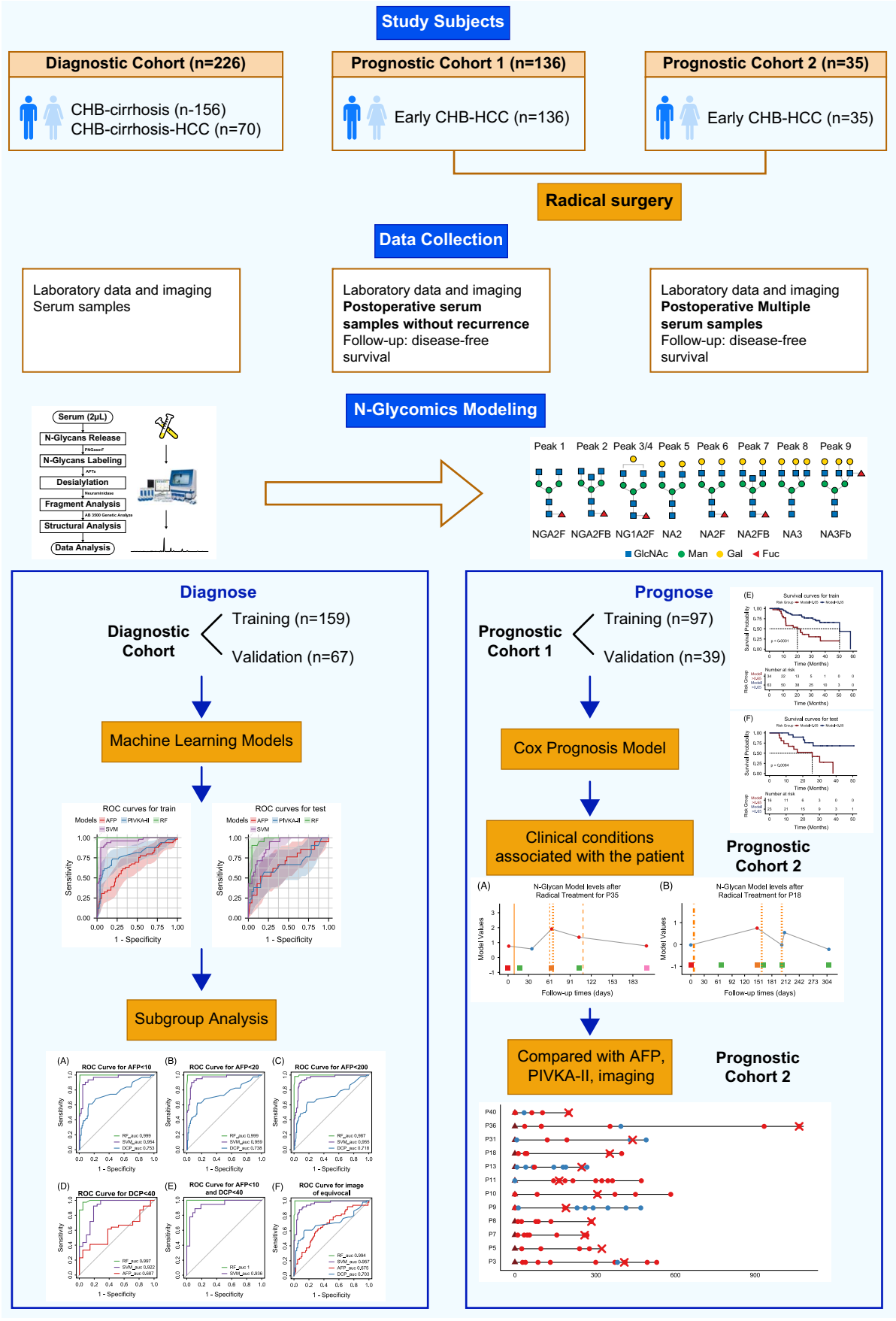
Study Subjects
Diagnostic Cohort (n=226)
CHB-cirrhosis (n-156)
CHB-cirrhosis-HCC (n=70)
Prognostic Cohort 1 (n=136)
Early CHB-HCC (n=136)
Prognostic Cohort 2 (n=35)
Early CHB-HCC (n=35)
Radical surgery
Data Collection
Laboratory data and imaging
Serum samples
Laboratory data and imaging
Postoperative serum samples without recurrence
Follow-up: disease-free survival
Laboratory data and imaging
Postoperative Multiple serum samples
Follow-up: disease-free survival
N-Glycomics Modeling
Serum (2μL)
N-Glycans Release
N-Glycans Labeling
Desialylation
Fragment Analysis
Structural Analysis
Data Analysis
Peak 1 Peak 2 Peak 3/4 Peak 5 Peak 6 Peak 7 Peak 8 Peak 9
NGA2F NGA2FB NG1A2F NA2 NA2F NA2FB NA3 NA3Fb
GlcNAc Man Gal Fuc
Diagnose
Diagnostic Cohort
Training (n=159)
Validation (n=67)
Machine Learning Models
ROC curves for train
ROC curves for test
Models AFP PIVKA-II RF SVM
Sensitivity
1 - Specificity
Subgroup Analysis
(A) ROC Curve for AFP<10
(B) ROC Curve for AFP<20
(C) ROC Curve for AFP<200
(D) ROC Curve for DCP<40
(E) ROC Curve for AFP<10 and DCP<40
(F) ROC Curve for image of equivocal
Prognose
Prognostic Cohort 1
Training (n=97)
Validation (n=39)
Cox Prognosis Model
Clinical conditions associated with the patient
Prognostic Cohort 2
(A) N-Glycan Model levels after Radical Treatment for P35
(B) N-Glycan Model levels after Radical Treatment for P18
Model Values
Follow-up times (days)
Compared with AFP, PIVKA-II, imaging
Prognostic Cohort 2
P40 P36 P31 P18 P13 P11 P10 P9 P8 P7 P5 P3
(E) Survival curves for train
(F) Survival curves for test
Survival Probability
Time (Months)
Number at risk
Risk Group

FIGURE 1 Outline of studies and study participants. Overview of the study design. A total of 397 individuals were included in the study, and their serum samples underwent targeted N-glycomics analysis. Abbreviations: AFP, alpha-fetoprotein; CHB, chronic hepatitis B; CHB-cirrhosis, chronic hepatitis B-related cirrhosis; CHB-cirrhosis-HCC, chronic hepatitis B-related cirrhosis and hepatocellular carcinoma; DFS, disease-free survival; HCC, hepatocellular carcinoma; NA2F, bigalacto core-α-1,6-fucosylated biantennary glycan; NA2FB, bigalacto core-α-1,6-fucosylated bisecting biantennary glycan; NA3F, branching α-1,3-fucosylated tri-antennary glycan; NA3FB, branching α-1,3-fucosylated bisecting tri-antennary glycan; NGA2F, agalacto core-α-1,6-fucosylated biantennary glycan; NGA2FB, agalacto core-α-1,6-fucosylated bisecting biantennary glycan; PIVKA-II, protein induced by vitamin K absence or antagonist-II; DSA-FACE, DNA sequencer-assisted fluorophore-assisted carbohydrate electrophoresis.

Prognostic cohort 2 was 11.76 (5.49-35.22) months, and the DFS rates were 72.58% and 56.92% at 1 year and 2 years, respectively. The median DFS of the patients was 35.2 months (95% CI: 14.6–not reached), and 12 patients reached the DFS endpoint. The survival curve for patients in cohort 2 is shown in Figure 2C.

Development of a ML diagnostic model for N-glycomics

Comparisons and modeling of N-glycan profiles in diagnostic cohort were conducted[20] (Supplemental Figure S2, Supplemental Digital Content 1, http://links.lww.com/HEP/J756 and Supplemental Table S3, Supplemental Digital Content 1, http://links.lww.com/HEP/J756). Comparisons of peaks 1–9 between patients with HCC and those without HCC are presented in Supplemental Table S4, Supplemental Digital Content 1, http://links.lww.com/HEP/J756, Supplemental Figure S3–S5, Supplemental Digital Content 1, http://links.lww.com/HEP/J756.

The total population was randomly divided into a training set (7:3, n = 159) and a validation set (n = 67) for subsequent model analysis (Supplementary Table S5, Supplemental Digital Content 1, http://links.lww.com/HEP/J756). Age, sex, and N-glycan peaks 1–9 of the training set (n = 159) were included in the logistic regression for univariate analysis (Figure 3A). The findings indicated that peak 1, peak 2, peak 6, peak 7, peak 8, and peak 9 exhibited statistically significant differences between groups ($p < 0.05$), which was consistent with the N-glycomics change data of the total population (n = 226).

We employed ML techniques—specifically RF and SVM—to construct 2 N-glycomics models [ie, Hepatocellular Carcinoma Glycomics Random Forest model (HCC-GRF) and Hepatocellular Carcinoma Glycomics Support Vector Machine model (HCC-GSVM)] based on the training set of 159 patients with $p < 0.1$ indicators (age, sex, peak 1, peak 2, peak 6, peak 7, peak 8, peak 9). The feature importance of the 2 constructed models is shown in Figures 3B, C.

The confusion matrix plots for HCC-GRF and HCC-GSVM are presented in Supplemental Figures 6A–D, Supplemental Digital Content 1, http://links.lww.com/HEP/J756. The AUCs for the training sets of the HCC-GRF and HCC-GSVM models were 1.000 (95% CI: 1.000–1.000) and 0.949 (0.912–0.986) ($p = 0.007$). For the validation set, the AUCs of the HCC-GRF and HCC-GSVM models were 0.967 (95% CI: 0.930–1.000) and 0.908 (0.840–0.976) ($p = 0.042$). Detailed performance metrics for the HCC-GRF, HCC-GSVM models, as well as for AFP and PIVKA-II are summarized in Table 1. The AUC values for AFP in the training set and validation set were 0.670 (95% CI: 0.575–0.765) and 0.687 (95% CI: 0.575–0.765), respectively, whereas those for PIVKA-II were 0.791 (95% CI: 0.706–0.876) and 0.665 (95% CI: 0.507–0.823), respectively. These findings indicated that the diagnostic performance of the 2 ML models established was significantly superior to that of AFP and PIVKA-II (Figures 3D, E). The calibration curve revealed that both models achieved good diagnostic performance in the validation set (Figures 3F, G). The DCA for the 2 models demonstrated a consistent net benefit in the training and validation sets over a range of threshold probabilities, which outperformed the "treat none" strategy, indicating that it had practical utility in decision-making (Figures 3H, I). The trends of sensitivity, specificity, PPV, and NPV for the HCC-GRF and HCC-GSVM models, as well as AFP and PIVKA-II at different thresholds on the training set and validation set, are illustrated in Supplemental Figures 6E, F, Supplemental Digital Content 1, http://links.lww.com/HEP/J756.

The performance of the N-glycomics diagnostic models in different subgroups

We compared the diagnostic performance of the HCC-GRF and HCC-GSVM models in patients with AFP < 10 ng/mL (n = 142), AFP < 20 ng/mL (n = 166), AFP < 200 ng/mL (n = 202), PIVKA-II < 40 mAU/mL (n = 166), AFP < 10 ng/mL and PIVKA-II < 40 mAU/mL (n = 129), imaging uncertainty (n = 135), and early HCC (n = 48). The AUC value of the HCC-GRF model clearly exceeded 0.980 in every subgroup, achieving a perfect score of 1 in the subgroup comprising patients with negative AFP and PIVKA-II (n = 129), with an optimal cutoff value of 0.455 identified for each subgroup. The AUC value of the HCC-GSVM surpassed 0.920 in various subgroups, thus indicating the superior suitability of HCC-GRF for diagnosing HBV-related HCC (Figure 4 and Supplemental Table S6, Supplemental Digital Content 1, http://links.lww.com/HEP/J756).

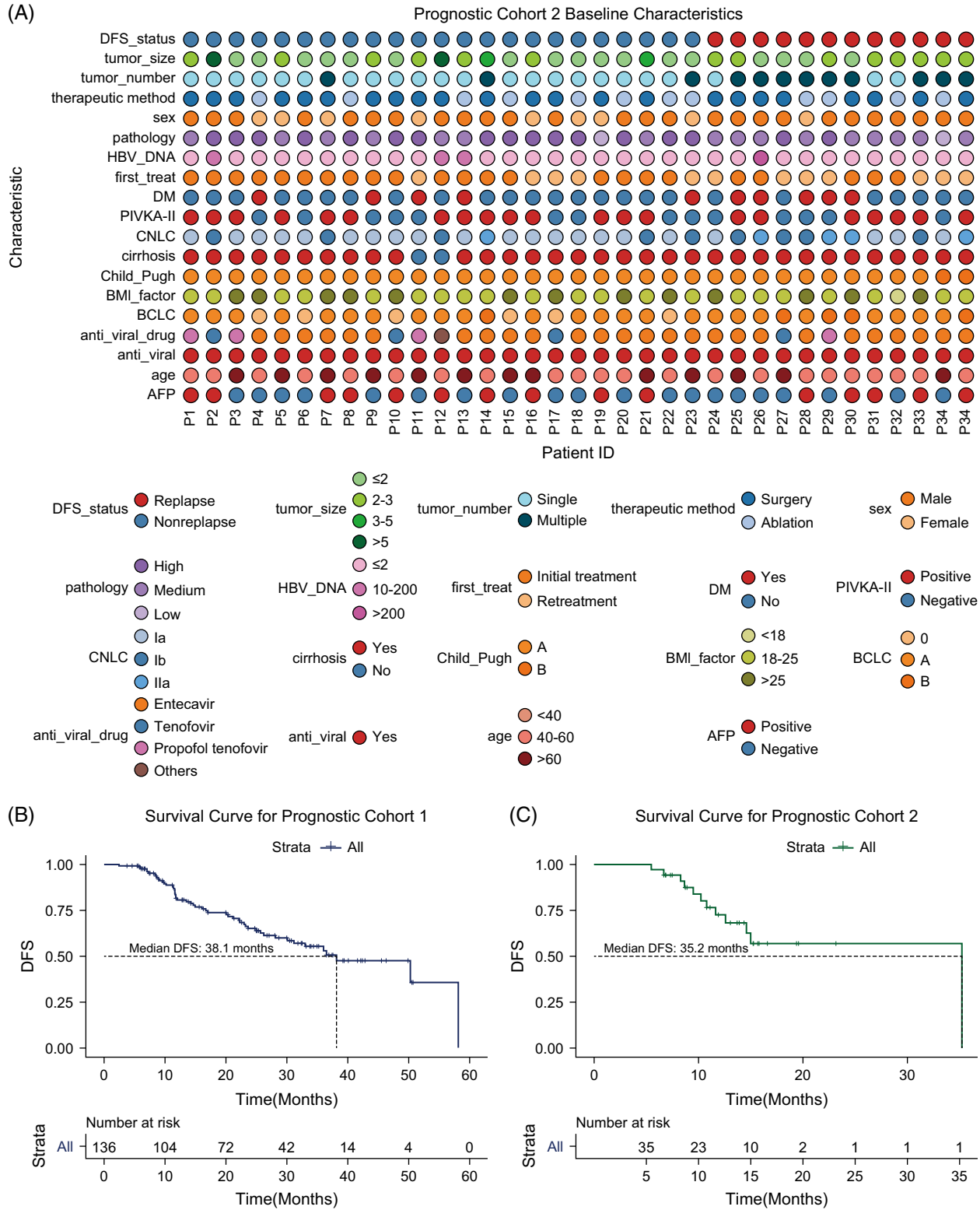

FIGURE 2 Clinical characteristics of the prognostic cohorts. (A) Baseline characteristics from prognostic cohort 2. (B) Survival curve for prognostic cohort 1. (C) Survival curve for prognostic cohort 2. Abbreviations: AFP, alpha-fetoprotein; anti_viral-drug, antiviral drug; BCLC, Barcelona Clinic Liver Cancer Staging; BMI_factor, body mass index factor; CHB, chronic hepatitis B; Child_Pugh, Child-Pugh liver function classification; CNLC, China Liver Cancer Staging System; DFS, disease-free survival; DSA-FACE, DNA sequencer-assisted fluorophore-assisted carbohydrate electrophoresis; DM, diabetes mellitus; HBV_DNA, hepatitis B virus deoxyribonucleic acid; PIVKA-II, protein induced by vitamin K absence or antagonist-II.

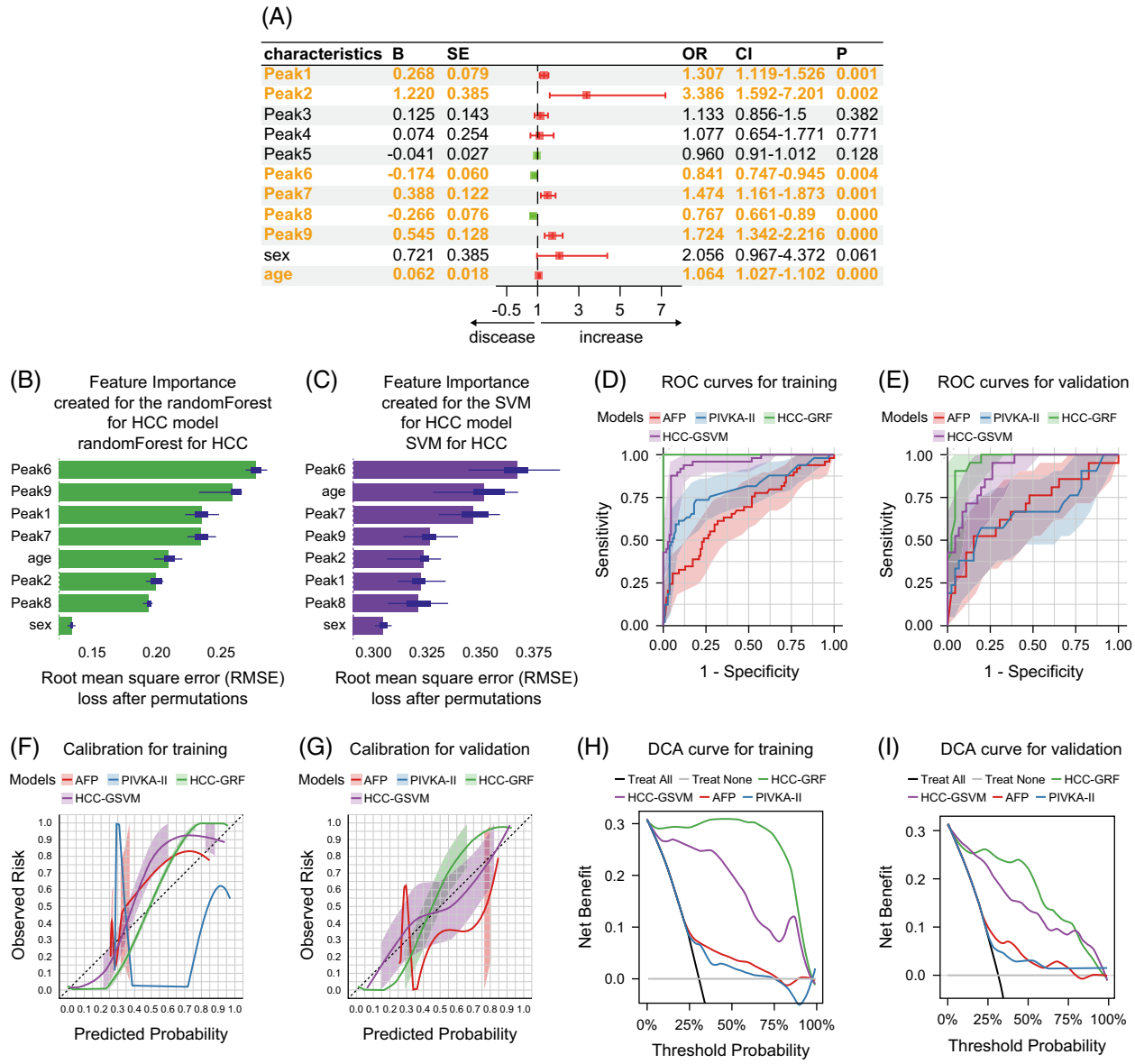

FIGURE 3 Machine learning-derived prediction model based on N-glycomics for HCC diagnosis. (A) Univariate logistic regression analysis of N-glycan peak 1–9 in the training set of the diagnostic cohort. (B, C) Variable importance of random forest model and support vector machine model in the training set of diagnostic cohort. (D, E) ROC curves of the 2 models, AFP and PIVKA-II, in the training and validation sets of the diagnostic cohort. (F, G) calibration curves of the 2 models, AFP and PIVKA-II, in the training and validation sets of the diagnostic cohort. (H, I) DCA curves of the 2 models, AFP and PIVKA-II, in the training and validation sets of the diagnostic cohort. Abbreviations: AFP, alpha-fetoprotein; PIVKA-II, protein induced by vitamin K absence or antagonist-II; HCC-GRF, hepatocellular carcinoma glycomics random forest model; HCC-GSVM, hepatocellular carcinoma glycomics support vector machine model; B, beta coefficient; SE, standard error; OR, odds ratio; CI, confidence interval; P, p-value; RF, random forest; SVM, support vector machine; ROC, receiver operating characteristic; DCA, decision curve analysis.

The performance of the N-glycomics diagnostic models in external validation

To further validate the performance of the 2 models, we enrolled 102 patients with CHB-cirrhosis, with or without HCC, from Beijing You'an Hospital as an external validation. Inclusion and exclusion criteria for all patients were consistent with those of our study population. Specifically, we included only patients with Barcelona Clinic Liver Cancer (BCLC) stage 0–B (BCLC 0: n = 16, BCLC A: n = 25, and BCLC B: n = 8). The external validation set comprised 49 patients with HCC and 53 patients without HCC. The AUC values of the HCC-GRF, HCC-GSVM, and AFP were 0.921 (95% CI: 0.869–0.974), 0.883 (95% CI: 0.820–0.946), and 0.688 (95% CI: 0.582–0.793), respectively (Supplemental Figure S7, Supplemental Digital Content 1, http://links.lww.com/HEP/J756 and Supplemental Table S7, Supplemental Digital Content 1, http://links.lww.com/HEP/J756).

TABLE 1 Diagnostic performance of HCC-GRF, HCC-GSVM, AFP, and PIVKA-II for patients with HCC in the diagnostic cohort

	AUC (95% CI)	Cutoff	SEN (%)	SPE (%)	ACC (%)	PPV (%)	NPV (%)	PLR	NLR
Training									
HCC-GRF	1.000 (1.000–1.000)	0.455	100.0	100.0	100.0	100.0	100.0	Inf	0.000
HCC-GSVM	0.949 (0.912–0.986)	0.385	87.8	95.5	93.1	89.6	94.6	19.306	0.272
AFP	0.670 (0.575–0.765)	8.940	61.2	68.2	66.0	46.2	79.8	1.924	0.569
PIVKA-II	0.791 (0.706–0.876)	33.500	73.5	80.9	78.6	63.2	87.3	3.848	0.328
Test									
HCC-GRF	0.931 (0.860–1.000)	0.455	90.5	95.7	94.0	90.5	95.7	20.810	0.100
HCC-GSVM	0.908 (0.840–0.976)	0.237	95.2	73.9	80.6	62.5	92.1	3.651	0.064
AFP	0.687 (0.575–0.765)	26.685	52.4	84.8	74.6	61.1	79.6	3.442	0.562
PIVKA-II	0.665 (0.507–0.823)	32.500	57.1	80.4	73.1	57.1	80.4	2.921	0.533
Total									
HCC-GRF	0.979 (0.950–1.000)	0.455	97.1	98.7	98.2	97.1	98.7	75.771	0.029
HCC-GSVM	0.939 (0.908–0.971)	0.237	94.3	82.7	86.3	71.0	97.0	5.448	0.069
AFP	0.676 (0.596–0.755)	9.225	58.6	70.5	66.8	47.1	79.1	1.986	0.791
PIVKA-II	0.756 (0.680–0.832)	32.500	68.6	80.1	76.5	60.8	85.0	3.451	0.392

Abbreviations: ACC, accuracy; AFP, alpha-fetoprotein; NLR, negative likelihood ratio; NPV, negative predictive value; PIVKA-II, abnormal prothrombin; PLR, positive likelihood ratio; PPV, positive predictive value; SEN, sensitivity; SPE, specificity.

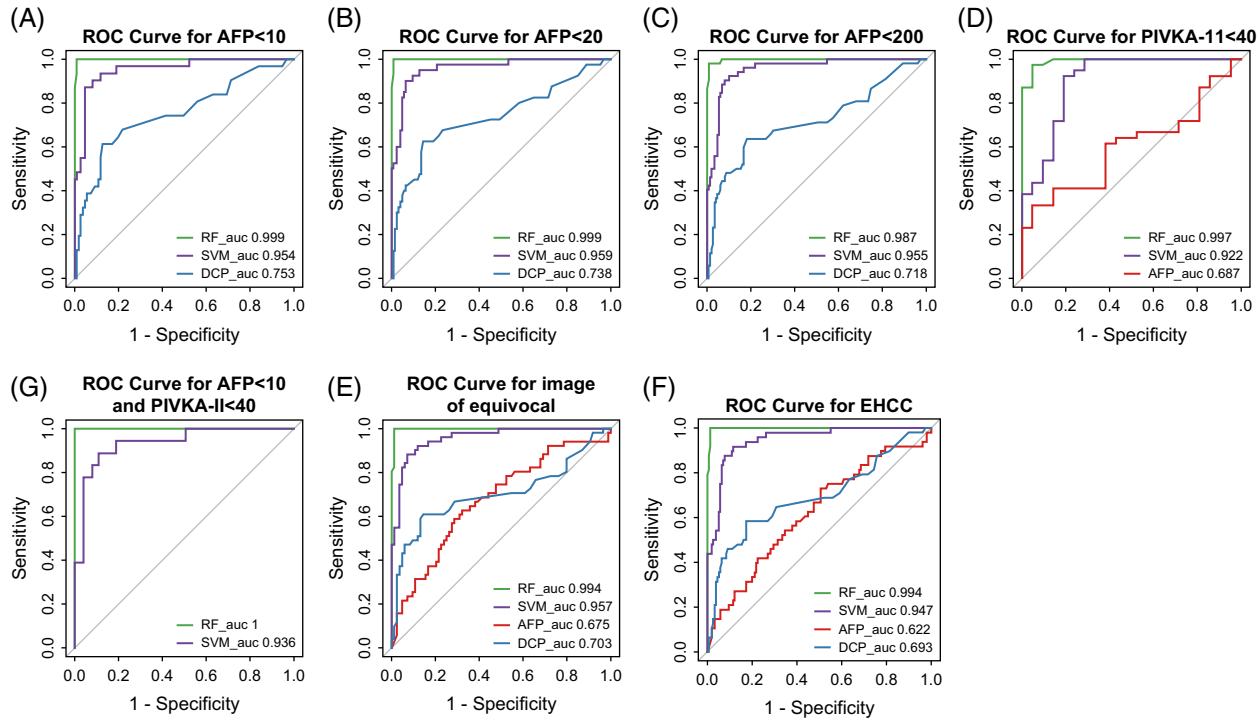

FIGURE 4 ROC curves of N-glycomics diagnostic models and common protein serum biomarkers in different subgroups. (A) ROC curves of machine learning models and common protein serum biomarkers in the population with AFP < 10 ng/mL. (B) ROC curves of machine learning models and common protein serum biomarkers in the population with AFP < 20 ng/mL. (C) ROC curves of machine learning models and common protein serum biomarkers in the population with AFP < 200 ng/mL. (D) ROC curves of machine learning models and common protein serum biomarkers in the population with PIVKA < 40 mAU/mL. (E) ROC curves of machine learning models and common protein serum biomarkers in the population with AFP < 10 ng/mL and PIVKA < 40 mAU/mL. (F) ROC curves of machine learning models and common protein serum biomarkers in the population with an image of equivocal. (G) ROC curves of machine learning models and common protein serum biomarkers in the population with early HCC. Abbreviations: AFP, alpha-fetoprotein; AUC, area under the ROC curve; DCP, des-γ-carboxy-prothrombin; EHCC, early hepatocellular carcinoma; PIVKA-II, protein induced by vitamin K absence or antagonist-II; RF, random forest; ROC, receiver operating characteristic; SVM, support vector machine; AFP < 10, AFP threshold at 10 ng/mL; AFP < 20, AFP threshold at 20 ng/mL; AFP < 200, AFP threshold at 200 ng/mL; PIVKA-II < 40, PIVKA-II threshold at 40 mAU/mL; RF_auc, random forest model AUC value; SVM_auc, support vector machine model AUC value; DCP_auc, des-γ-carboxy-prothrombin AUC value.

Development of a prognostic model for N-glycomics

Following rigorous standardization, the N-glycan profile was utilized to assess DFS using Cox univariate regression analysis (Figure 5A). In this analysis, the *p* values of 8 N-glycans (peak 1, peak 2, peak 3, peak 5, peak 6, peak 7, peak 8, and peak 9) were < 0.1.

Prognostic cohort 1 was stratified into a training set (n = 97) and a validation set (n = 39) through a rigorous random sampling approach with an allocation ratio of 7:3 (Supplemental Table S8, Supplemental Digital Content 1, http://links.lww.com/HEP/J756). The eight N-glycans ($p < 0.1$) identified through univariate analysis were selected as predictive markers for the model. A prognostic model based on the N-glycan profile was subsequently developed using the Cox regression method in the training set to assess the risk of postoperative recurrence in patients with early HCC: model = 1.1513 × peak 1 − 0.1980 × peak 2 + 0.3732 × peak 3 + 0.4115 × peak 5 − 0.2461 × peak 6 + 1.3921 × peak 7 − 0.4359 × peak 8 + 0.5779 × peak 9. The model was named the prog-G model.

To apply the prog-G model in clinical practice, the postoperative follow-up time of the enrolled patients was combined, and the ROC curve was examined to determine the optimal cutoff value of the N-glycan model for predicting recurrence within 2 years after curative treatment.[26] The optimal cutoff value was 0.65. Based on this cutoff value, the patients in the training set and validation set were divided into high-risk groups and low-risk groups for further analysis. The ROC curves of the training set, validation set, and total population for predicting recurrence within 2 years are shown in Figures 5B–D, with AUC values of 0.798 (95% CI: 0.692–0.904), 0.707 (95% CI: 0.485–0.930), and 0.769 (95% CI: 0.671–0.867), respectively (Supplemental Table S9, Supplemental Digital Content 1, http://links.lww.com/HEP/J756). According to the univariate Cox analysis, the treatment method, initial treatment status, BCLC stage, CNLC stage, postoperative AFP, and the prog-G model were found to be significant predictors of DFS, but only the prog-G model exhibited significant differences among the 3 groups. Multivariate analysis revealed that the prog-G model was an independent predictor of HCC recurrence risk after surgery. Survival curve analysis (Figures 5E–G and Supplemental Figure S8, Supplemental Digital Content 1, http://links.lww.com/HEP/J756) revealed that DFS was significantly shorter in the high-risk group than in the low-risk group, based on the cutoff value of the N-glycan model (0.65).

Correlation of the prog-G model with patients' clinical conditions

To explore the association between the prog-G model and the clinical condition of patients, N-glycomics analysis was conducted on serum samples collected at various time points following curative treatment in Prognostic cohort 2. The dynamic changes in the N-glycan prognostic model were monitored (Supplemental Table S10, Supplemental Digital Content 1, http://links.lww.com/HEP/J756). Recurrence was determined by 2 senior chief physicians based on imaging results, serum biological protein markers, and clinical status.

Trend of the prog-G model in recurrent patients

A total of 12 patients experienced recurrence during the follow-up period following surgery. Among these patients, those identified as P24, P25, P26, P27, P28, P29, P30, P31, P32, P13, and P35 experienced recurrence within 2 years postsurgery, whereas patient P34 experienced recurrence after a period exceeding 2 years. Patient P35 (Figure 6A) had a positive prog-G model before surgery and underwent hepatectomy, after which the patient's prog-G model became negative. However, the model reverted to a positive state at 55 days postsurgery, and imaging failed to confirm HCC recurrence. The model remained positive on 2 further occasions until the patient was confirmed to have HCC recurrence at 194 days postsurgery, indicating that the prog-G model is closely related to the recurrence time of the patient.

Trend of the prog-G model in patients without recurrence

A total of 23 patients experienced no recurrence during the follow-up period. Among these patients, patient P15 demonstrated a persistently negative prog-G model throughout the follow-up period, which was consistent with their clinical condition (Supplemental Files, Supplemental Digital Content 1, http://links.lww.com/HEP/J756). Patient P18 had a positive N-glycomics model 141 days after surgery and underwent TACE treatment 151 days after surgery, with a negative N-glycan model 196 days after surgery, indicating that the patient's clinical condition was closely related to the change in N-glycomics (Figure 6B). Patients P23, P9, and P19 had negative glycan models after curative treatment but were positive at 147 days, 50 days, and 187 days after follow-up, respectively; however, there was no clinical indication of HCC recurrence at present, and the follow-up time of all 3 patients was < 1 year. They need to be followed up regularly and closely monitored for changes in their condition. Patients P13, P14, P15, and P17 had persistently positive N-glycomics models during follow-up. Upon reviewing the medical records, four patients lacked abdominal CT or MRI results, and only blood serum and abdominal ultrasound examinations were performed every 3–6 months at our hospital.

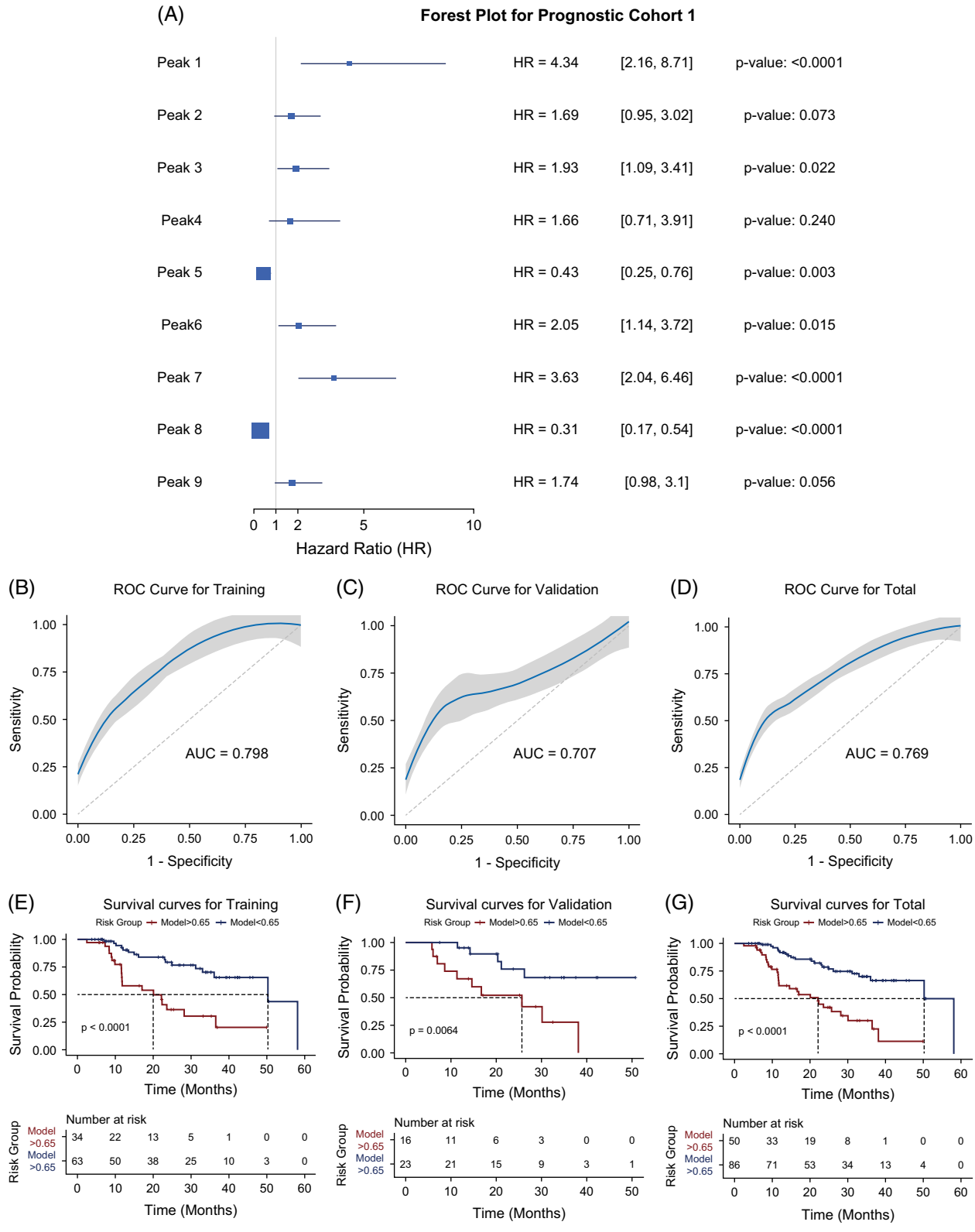

FIGURE 5 Forest plot, ROC curves, and survival curves in prognostic cohort 2. (A) Univariate Cox regression analysis of N-glycan peak 1–9 in prognostic cohort 1. (B–D) ROC curves of the training set, validation set, and total population according to whether the recurrence occurred within 2 years of prognostic cohort 1. (E–G) Survival curves for training, validation and total set of prognostic cohort 1. Abbreviations: AUC, area under the ROC curve; HR, hazard ratio; ROC, receiver operating characteristic; CI, confidence interval.

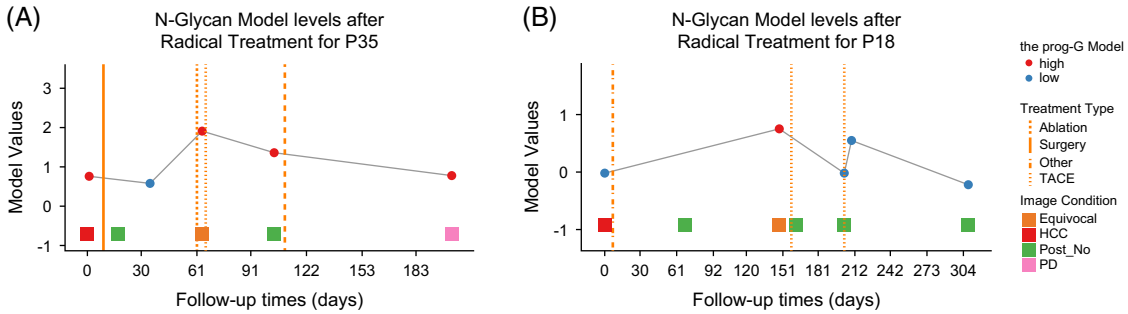
(A)
N-Glycan Model levels after Radical Treatment for P35
Model Values
Follow-up times (days)
(B)
N-Glycan Model levels after Radical Treatment for P18
Model Values
Follow-up times (days)
the prog-G Model
high
low
Treatment Type
Ablation
Surgery
Other
TACE
Image Condition
Equivocal
HCC
Post_No
PD

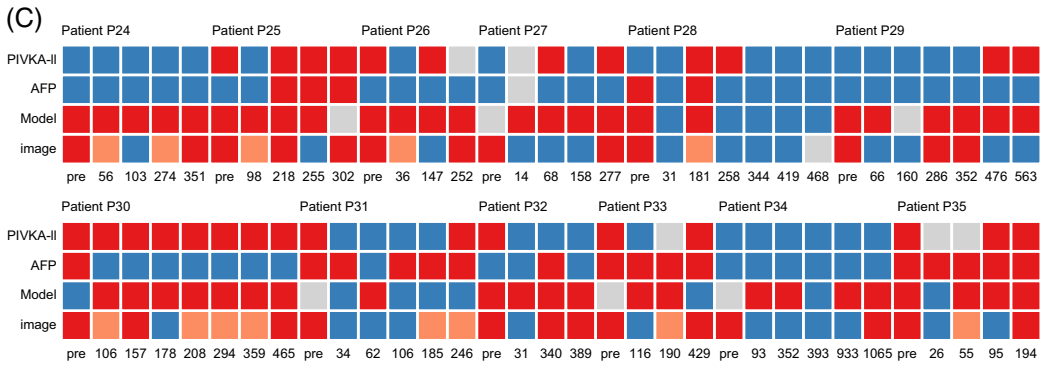
(C)
Patient P24
Patient P25
Patient P26
Patient P27
Patient P28
Patient P29
Patient P30
Patient P31
Patient P32
Patient P33
Patient P34
Patient P35
PIVKA-II
AFP
Model
image

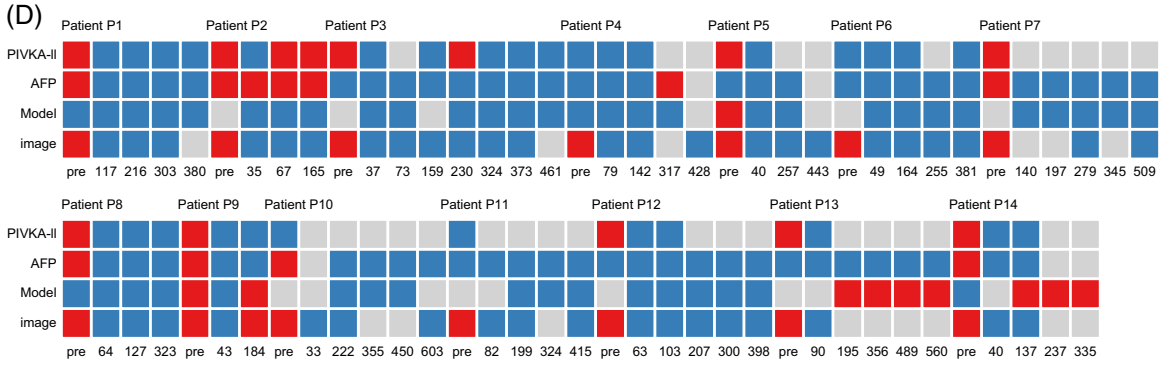
(D)
Patient P1
Patient P2
Patient P3
Patient P4
Patient P5
Patient P6
Patient P7
Patient P8
Patient P9
Patient P10
Patient P11
Patient P12
Patient P13
Patient P14
Patient P15
Patient P16
Patient P17
Patient P18
Patient P19
Patient P20
Patient P21
Patient P22
Patient P23
PIVKA-II
AFP
Model
image
Positive
Negative
Equivocal
Unknown

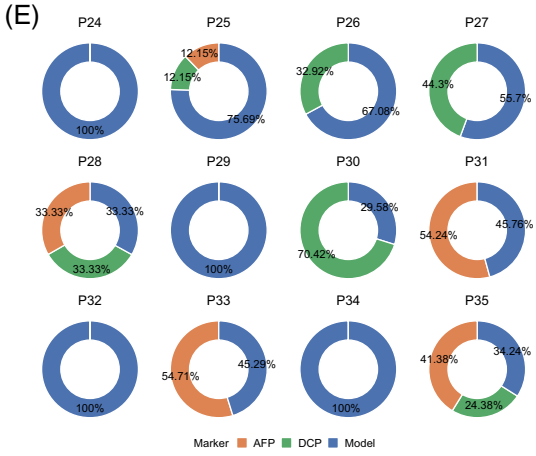
(E)
P24
P25
P26
P27
P28
P29
P30
P31
P32
P33
P34
P35
Marker AFP DCP Model

FIGURE 6 Comparison of N-glycomics prognostic models and protein biomarkers for HCC surveillance. (A, B) Patients P35 and P18 in prognostic cohort 2 during the entire follow-up period after radical surgery. The horizontal axis represents the time of postoperative follow-up, and the dots represent the glycomics model values tested, with blue indicating no recurrence and red indicating recurrence (see the Supplemental Material for follow-up maps of all patients). (C, D) The categorization of imaging results, glycomics model status, and serum biomarker (AFP and PIVKA-II) results during each patient's clinical course are shown in each color-code plot. Red indicated positive, yellow indicated equivocal, while blue indicated negative. (E) The proportion of the time of HCC recurrence detected earlier by glycomics model, AFP, and PIVKA-II than imaging, respectively. Abbreviations: AFP, alpha-fetoprotein; DCP: des-γ-carboxy-prothrombin; N-Glycan Model, serum N-linked glycan prognostic model; PIVKA-II, protein induced by vitamin K absence or antagonist-II; pre, pretreatment; P[number], patient identifier.

Future research should focus on the prognosis of these 4 patients. One reason that the negative prog-G model was not completely consistent with patients without recurrence might be that the N-glycomics model can detect invisible tumors before imaging.

Comparison of the prog-G model with serum biomarkers and imaging data

In this study, we collected multiple AFP, PIVKA-II, and corresponding serological samples from patients in prognostic cohort 2 at our hospital and conducted N-glycomics analysis to compare the performance of the prog-G model with that of AFP and PIVKA-II in monitoring the prognosis of patients with HCC. The cutoff levels of AFP and PIVKA-II were 20 ng/mL and 40 mAU/mL, respectively.

Comparison of the prog-G model, AFP, and PIVKA-II in relapsed patients

The changes in the postoperative N-glycan model, AFP, and PIVKA-II over time in the 12 recurrent patients are shown in Figure 7 and Supplemental Figures 9, 10, Supplemental Digital Content 1, http://links.lww.com/HEP/J756. To compare the changes in the prog-G model, AFP, and PIVKA-II more clearly, we categorized the status of the prog-G model, AFP, PIVKA-II, and imaging examinations in each patient with similar collection times to assess the performance of the prog-G model, AFP, and PIVKA-II in HCC prognostic monitoring (Figure 6C). All 12 patients clearly presented positive results at the postoperative follow-up of the prog-G model, whereas P24, P26, P27, P29, and P34 consistently presented negative AFP results. Additionally, P24, P32, and P34 consistently demonstrated negative PIVKA-II results during the entire follow-up duration. These findings suggested that the prog-G model significantly outperformed AFP and PIVKA-II in terms of predicting the trajectory of HCC recurrence.

Comparison of the prog-G model, AFP, and PIVKA-II in nonrelapsed patients

For the 23 patients without recurrence, the postoperative changes in the N-glycan model, AFP, and PIVKA-II over time are shown in Figure 7, Supplemental Figures 9, 10, Supplemental Digital Content 1, http://links.lww.com/HEP/J756, and Figure 6D. During follow-up, the N-glycan model detected more positive results than AFP and PIVKA-II did in predicting HCC recurrence, suggesting that the N-glycan model may be more sensitive to HCC than AFP and PIVKA-II. During follow-up, patients P23, P9, P13, P14, P15, P17, P18, and P19 had positive prog-G model results; patients P7, P2, P4, P15, and P18 had positive AFP results; and patients P7, P2, P3, P15, and P17 had positive PIVKA-II results. Patient P15 had positive results for the prog-G model, AFP, and PIVKA-II during follow-up, with only one negative imaging result and one intervention during postoperative treatment.

The prog-G model detected HCC recurrence after surgery earlier than the imaging

Next, we compared the N-glycan prognostic model with imaging examinations to predict HCC recurrence, and found that the N-glycan prognostic model could predict recurrence earlier than imaging examinations, AFP, and PIVKA-II (Supplemental Table S9, Supplemental Digital Content 1, http://links.lww.com/HEP/J756). Among the 12 patients who experienced recurrence, 10 had clear imaging evidence of HCC recurrence, while the prog-G model was shown to predict HCC recurrence earlier based on prerecurrence samples in all cases. Overall, the sensitivity of the prog-G model in detecting recurrence in patients was 100% (12/12), whereas only 5 out of 12 cases of recurrence could be detected by AFP, with a sensitivity of 41.67% (5/12), and only 6 out of 12 cases of recurrence could be detected by PIVKA-II, with a sensitivity of 50% (6/12). The prog-G model often detected the risk of recurrence in patients earlier than AFP and PIVKA-II, thus indicating the sensitivity of the prog-G model in screening for HCC recurrence (Supplemental Table S11, Supplemental Digital Content 1, http://links.lww.com/HEP/J756 and Figure 6E). These results proved that our model could serve as a novel and sensitive method for identifying residual microtumors and the risk of recurrence.

DISCUSSION

In this study, we developed and validated diagnostic and prognostic models for CHB-related HCC based on

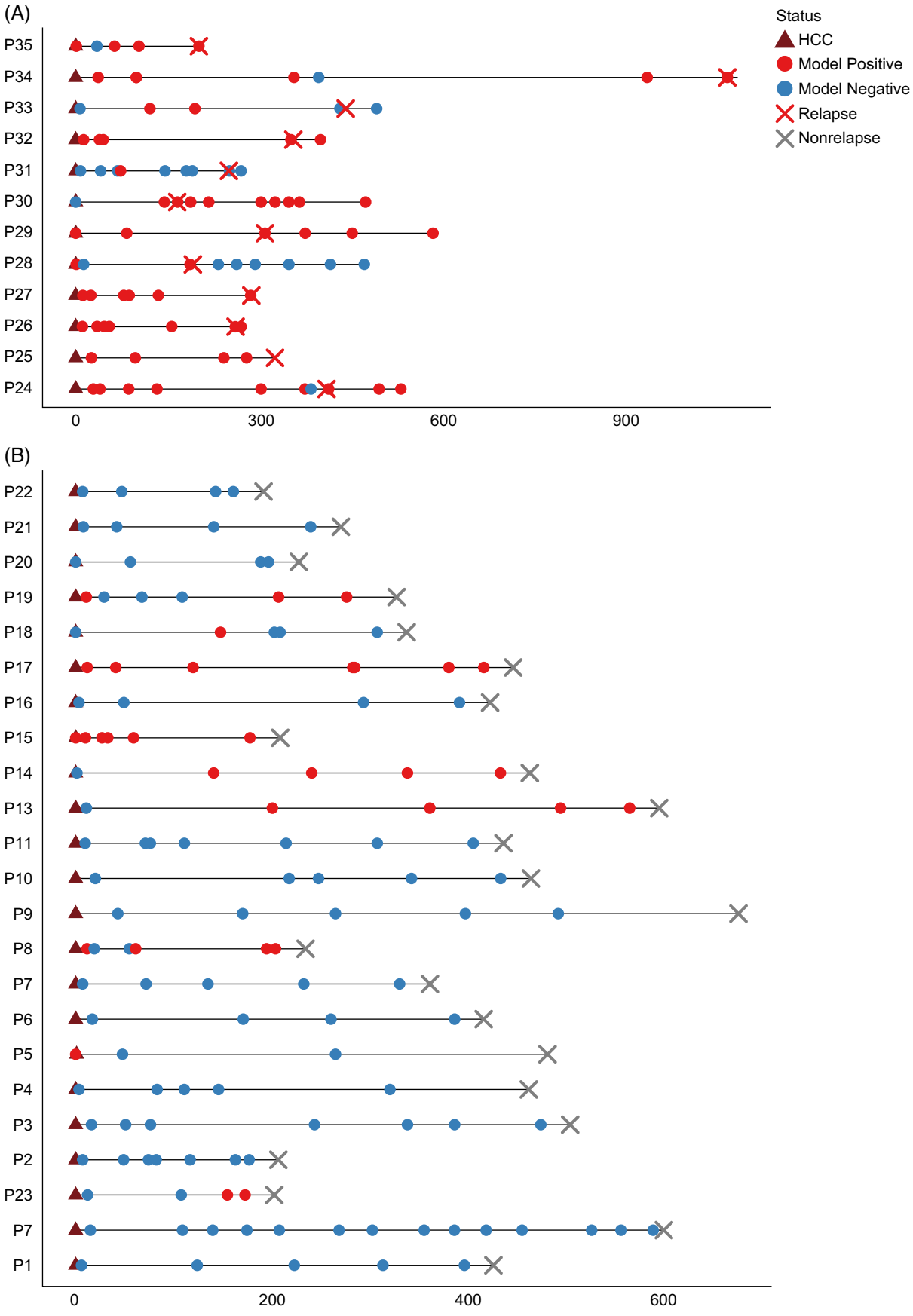
(A)
P35
P34
P33
P32
P31
P30
P29
P28
P27
P26
P25
P24
0
300
600
900
Status
HCC
Model Positive
Model Negative
Relapse
Nonrelapse
(B)
P22
P21
P20
P19
P18
P17
P16
P15
P14
P13
P11
P10
P9
P8
P7
P6
P5
P4
P3
P2
P23
P7
P1
0
200
400
600

FIGURE 7 The timeline presentation of the N-glycomics model status and clinical outcomes. (A) The timeline presentation of the glycomics model status and clinical outcomes in relapsed patients in prognostic 2. (B) The timeline presentation of the glycomics model status and clinical outcomes in nonrelapsed patients in prognostic 2. Abbreviation: HCC, hepatocellular carcinoma.

N-glycomics. Specifically, we initially utilized ML to analyze N-glycomics data and developed the HCC-GRF and HCC-GSVM models, which exhibited superior diagnostic performance compared with standard serum biomarkers. Subgroup analysis and external validation were also performed to improve predictive accuracy. Furthermore, we formulated a Cox prognostic model, the prog-G model, for patients with CHB-related HCC who underwent curative treatment. This model was correlated with the clinical status of these patients following multiple postoperative follow-ups and outperformed HCC prognostic serum biomarkers by enabling earlier detection of HCC recurrence than imaging findings. In summary, our study highlights the distinct advantages of N-glycomics in terms of facilitating early detection and precision medicine for the treatment of HCC. The model developed herein holds promise for future clinical translation.

The low long-term survival rate of HCC is mainly due to low rates of early diagnosis and high rates of recurrence after treatment.[5,27,28] According to statistics, the 2-year recurrence rate of HCC patients after curative treatment is 30%–50%, and the 5-year recurrence rate may exceed 70%. The earliest time for recurrence may be 2 months after surgery, and the peak may occur within 1–2 years after surgery, which significantly affects the long-term survival rate of patients.[29,30] Hence, there is an imperative need to develop noninvasive methods for early screening and recurrence monitoring, enhance precision medicine guidance, and prolong patient survival duration. In previous research on biomarkers for HCC using omics technologies, the focus was mainly on liquid biopsy, proteomics, and imaging genomics.[9,31–34] Although various common omics technologies have undergone certain developments, they still face problems such as low sensitivity and high cost. For example, liquid biopsy ctDNA for early or low-load tumors may have very low concentrations of ctDNA, have limited detection sensitivity and are expensive. Glycomics, a less commonly used omics technology, has also been increasingly used in the diagnosis of liver disease and other diseases in recent years.[35–37] Disruption of liver homeostasis leads to the upregulation or downregulation of enzymes involved in the production of N-glycan end products in hepatocytes. Therefore, changes in the protein glycoproteins in the serum may reflect the destruction of liver function.[35,38] Serum N-glycan analysis using DNA sequencer-assisted fluorophore-assisted carbohydrate electrophoresis technology has been proven to be both feasible and reliable. Only 2 μL of serum sample are required for this analysis, and the detection process time is significantly reduced to 6 hours.[39] Previous studies have shown that changes in serum N-glycan levels can be used to monitor the progression of fibrosis, cirrhosis, and HCC, and specific N-glycan markers can be used to predict the onset of disease.[20,21,40,41] However, few studies have used ML algorithms to establish N-glycomics models for diagnosing HCC, and even fewer have focused on the role of N-glycan changes in predicting recurrence among patients with HCC after surgery. N-glycans, as a form of glycosylation, exhibit specific changes in their alterations (such as an increase in branching structures or the appearance of specific glycans) that can reflect changes in the tumor microenvironment and in the behavior of tumor cells. These changes may be used to monitor tumor recurrence and evaluate the effectiveness of treatment.[42,43] Hence, there is a possibility of tracking the dynamic changes in residual tumor lesions by regularly monitoring specific glycosylation patterns.

Our study focused on N-glycomics to investigate glycomic changes in patients with CHB-related cirrhosis with or without HCC, and to establish relevant diagnostic models. Our findings revealed that 6 glycopeaks (peak 1: agalacto core-α-1,6-fucosylated biantennary glycan, NGA2F; peak 2: agalacto core-α-1,6-fucosylated bisecting biantennary glycan, NGA2FB; peak 6: bigalacto core-α-1,6-fucosylated biantennary glycan, NA2F; peak 7: bigalacto core-α-1,6-fucosylated bisecting biantennary glycan, NA2FB; peak 8: triantennary glycan, NA3; peak 9: branching α-1,3-fucosylated triantennary glycan, NA3Fb) exhibited statistically significant differences between the 2 groups, consistent with the peaks identified in previous studies by Liu et al [20] and Cong et al.[21] Previous research[44] has also indicated that an abnormal increase in NA3Fb occurs early in HCC development and is age-independent. Moreover, changes in the core α−1,6-fucosylation of triantennary glycan chains in the serum and tissues of patients with HCC may reflect molecular mechanisms during cancer progression and could serve as novel tumor-associated antigens or drug targets. We subsequently developed the HCC-GRF and HCC-GSVM models using RF and SVM, respectively, within the training set. In terms of sensitivity, specificity, PPV, and NPV for diagnostic performance within both the training set and validation set, the 2 models demonstrated clear advantages over the traditional tumor markers AFP and PIVKA-II. Notably, in the validation set, the AUC value of the HCC-GRF model reached 0.967, indicating strong discriminatory ability and accuracy. These findings suggest that glycomics-based ML models, particularly the RF model, exhibit remarkable stability

and precision in discriminating between cirrhotic patients with or without HCC, thus providing a novel approach to enhancing early HCC diagnosis in clinical practice. Moreover, the stability and validity of the models are also demonstrated in subgroup analysis and external validation. These findings underscore the clinical significance of the glycomic model in HCC diagnosis as a crucial clinical biomarker that enhances sensitivity and specificity in HCC detection while reducing missed diagnosis rates.[40]

We further explored the potential of N-glycomics for monitoring recurrence in patients with HCC associated with CHB after curative treatment. A prognostic model, the prog-G model, was developed to predict HCC recurrence and was validated via Cox regression analysis. The parameters of the model were adjusted based on whether the patients had experienced recurrence by the end of follow-up. The identified sugar peaks consisted of peak 1, peak 2, peak 3 (single agalacto core-α-1,6-fucosylated biantennary glycan, NGA2FB), peak 5 (bigalacto biantennary glycan, NA2), peak 6, peak 7, peak 8, and peak 9. Gui et al [41] demonstrated a significant decrease in the N-glycans of NA2 and NA3 with increasing fibrosis severity. Nie et al[44] reported reduced levels of NA2 and NA3 in the serum of patients with HCC. These findings suggest that the decrease in NA2 and NA3 in the serum is decreased in more severe stages of liver disease, which is consistent with our results. NA3Fb has been consistently associated with HCC in multiple studies.[20,40,44] In our study, both the diagnostic and prognostic models for HCC included NA3Fb, which aligns with previous findings. β1,6-GlcNAc-branched glycans of CD147/basigin by N-acetylglucosaminyltransferase V (GnT-V) upregulated the expression of matrix metalloproteinases (MMPs) (eg, MMP-1, MMP-2, and MMP-9) and enhanced their associations with integrin β1, thereby contributing to HCC metastasis.[45,46] In addition, N-acetylglucosaminyltransferase IVa can upregulate the specific N-glycan branch-α-1,3-fucosylated triantennary glycan (NA3Fb) on the surface of malignant hepatocytes, promoting the migration and invasion of HCC cells.[44] In prognostic cohort 2 (n = 35), we observed a significant association between the prog-G model and the postsurgical clinical status of patients, as well as a close correlation between the N-glycan model and the receipt of postsurgical treatments (eg, TACE, immune-targeted therapy) and recurrence. Notably, the prog-G model exhibited positive results in all relapsed patients (n = 12) earlier than imaging evidence revealed HCC recurrence. Our findings showed that N-glycomics have the potential to detect microtumor residual lesions, enabling early monitoring of HCC recurrence postsurgery and highlighting the pivotal role of glycosylation in tumor progression.[47] Furthermore, comparison with other protein biomarkers (AFP and PIVKA-II) underscored the superior performance of the glycomic model. In nonrelapsed patients (n = 23), compared with AFP, PIVKA-II, and imaging examinations, the prog-G model demonstrated greater positivity, thus indicating its potential for early detection of postoperative recurrent lesions.[47,48]

Although this study successfully established and validated glycomic models for early detection and recurrence monitoring of HCC, it also has some limitations. However, this study has certain limitations. First, the single-center design may restrict the generalizability and applicability of the model. Future research should consider multicenter collaboration to gather glycomic samples from patients in diverse geographic regions and with varied medical backgrounds for analysis and validation. Second, in recurrence monitoring studies, incomplete collection of some serum samples resulted in a lack of complete correspondence between glycomics, AFP, PIVKA-II, and imaging examination timing; additionally, irregular patient follow-up was observed. Furthermore, despite significant progress in the early screening and diagnosis of CHB-related HCC as well as recurrence management through glycomic analysis, the underlying biological mechanisms driving these changes remain incompletely understood. Therefore, future research needs to delve deeper into the biological significance and mechanism of action of these glycomic markers.

In conclusion, this study illustrated the potential of N-glycomics in early screening, diagnosis, and postoperative follow-up monitoring of HCC in CHB-related patients, presenting objective and empirical evidence. The diagnostic and prognostic models we have devised can accurately and sensitively anticipate the onset of HCC as well as predict its recurrence following curative treatment, thereby enhancing the efficacy of clinical decision-making and personalized management for postsurgery HCC patients while contributing to improved patient prognosis.

DATA AVAILABILITY STATEMENT

We are unable to provide access to our data set for privacy reasons. The protocol and statistical analysis methods used in the study can be requested directly from the corresponding author after approval.

AUTHOR CONTRIBUTIONS

Rui Su, Liang Xu, Xuemei Tao, and Yuqiang Mi designed the study; Xuemei Tao, Rui Su, Lihua Yan, and Liang Xu performed the research; Yonggang Liu, Ping Li, Jia Li, Jing Miao, Feng Liu, and Jiancun Hou provided the clinical and pathological data; Xuemei Tao, Lihua Yan, and Wentao Kuai collected data; Cuiying Chitty Chen performed the N-glycomics analysis; Xuemei Tao and Cuiying Chitty Chen carried out statistical analysis; Xuemei Tao, Rui Su, and Liang Xu wrote the manuscript; Xuemei Tao, Rui Su, Liang Xu,

and Yuqiang Mi critical revised of the manuscript. All the authors have read and approved the final revision to be published.

FUNDING INFORMATION

This work was supported by the National Natural Science Foundation of China (62375202), National Science and Technology Major Project (No.2023ZD0508702), Natural Science Foundation of Tianjin (23JCYBJC00950), Tianjin Health Science and Technology Project key discipline special (TJWJ2022XK034), Tianjin Key Medical Discipline (Specialty) Construction Project (TJYXZDXK-059B), Research project in key areas of TCM in 2024 (2024022). Noncommunicable Chronic Diseases-National Science and Technology Major Project (No.2023ZD0508702).

CONFLICTS OF INTEREST

The authors have no conflicts to report.

ORCID

Xuemei Tao https://orcid.org/0000–0003–1245–0343
Liang Xu https://orcid.org/0000–0001–5441–1217

References

1. Bray F, Laversanne M, Sung H, Ferlay J, Siegel RL, Soerjomataram I, et al. Global cancer statistics 2022: GLOBOCAN estimates of incidence and mortality worldwide for 36 cancers in 185 countries. CA Cancer J Clin. 2024;74:229–63.
2. Liu H, Wang X, Wang L, Yin P, Liu F, Wei L, et al. Mortality burden of liver cancer in China: An observational study from 2008 to 2020. J Clin Transl Hepatol. 2024;12:371–80.
3. Timmerman R. A story of hypofractionation and the table on the wall. Int J Radiat Oncol Biol Phys. 2022;112:4–21.
4. Toh MR, Wong EYT, Wong SH, Ng AWT, Loo LH, Chow PKH, et al. Global epidemiology and genetics of hepatocellular carcinoma. Gastroenterology. 2023;164:766–82.
5. McMahon B, Cohen C, Brown RS Jr, El-Serag H, Ioannou GN, Lok AS, et al. Opportunities to address gaps in early detection and improve outcomes of liver cancer. JNCI Cancer Spectr. 2023;7:pkad034.
6. Saito A, Toyoda H, Kobayashi M, Koiwa Y, Fujii H, Fujita K, et al. Prediction of early recurrence of hepatocellular carcinoma after resection using digital pathology images assessed by machine learning. Mod Pathol. 2021;34:417–25.
7. Singal AG, Kanwal F, Llovet JM. Global trends in hepatocellular carcinoma epidemiology: implications for screening, prevention and therapy. Nat Rev Clin Oncol. 2023;20:864–84.
8. Hao X, Deng SY, Wang KY, Chen L, Hou JL, Wei WW, et al. Application of liquid biopsy in early screening and recurrence prediction of hepatocellular carcinoma. J Hepatol. 2022;30:814–9.
9. Cai Z, Chen G, Zeng Y, Dong X, Li Z, Huang Y, et al. Comprehensive liquid profiling of circulating tumor DNA and protein biomarkers in long-term follow-up patients with hepatocellular carcinoma. Clin Cancer Res. 2019;25:5284–94.
10. Wang W, Wei C. Advances in the early diagnosis of hepatocellular carcinoma. Genes Dis. 2020;7:308–19.
11. Rudd PM, Elliott T, Cresswell P, Wilson IA, Dwek RA. Glycosylation and the Immune System. Science [Internet]. 2001;291:2370–6.
12. Beltrao P, Albanèse V, Kenner LR, Swaney DL, Burlingame A, Villén J, et al. Systematic functional prioritization of protein posttranslational modifications. Cell. 2012;150:413–25.
13. Wang J, Liu J, Li M, Wang Y, Man Q, Zhang H, et al. Novel three-dimensional hierarchical porous carbon probe for the discovery of N-Glycan biomarkers and early hepatocellular carcinoma detection. Anal Chem. 2023;95:10231–40.
14. Pinho SS, Reis CA. Glycosylation in cancer: Mechanisms and clinical implications. Nat Rev Cancer. 2015;15:540–55.
15. Hu M, Zhang R, Yang J, Zhao C, Liu W, Huang Y, et al. The role of N-glycosylation modification in the pathogenesis of liver cancer. Cell Death Dis. 2023;14:1–12.
16. Jiang K, Li W, Zhang Q, Yan G, Guo K, Zhang S, et al. GP73 N-glycosylation at Asn144 reduces hepatocellular carcinoma cell motility and invasiveness. Oncotarget. 2016;7:23530–41.
17. Liu Y, Lan L, Li Y, Lu J, He L, Deng Y, et al. N-glycosylation stabilizes MerTK and promotes hepatocellular carcinoma tumor growth. Redox Biol. 2022;54:102366.
18. Callewaert N, Geysens S, Molemans F, Contreras R. Ultra-sensitive profiling and sequencing of N-linked oligosaccharides using standard DNA-sequencing equipment. Glycobiology. 2001;11:275–81.
19. Cao X, Shang QH, Chi XL, Zhang W, Xiao HM, Sun MM, et al. Serum N-glycan markers for diagnosing liver fibrosis induced by hepatitis B virus. World J Gastroenterol. 2020;26:1067.
20. Liu XE, Desmyter L, Gao CF, Laroy W, Dewaele S, Vanhooren V, et al. N-glycomic changes in hepatocellular carcinoma patients with liver cirrhosis induced by hepatitis B virus. Hepatology. 2007;46:1426–35.
21. Cong M, Ou X, Huang J, Long J, Li T, Liu X, et al. A predictive model using N-Glycan biosignatures for clinical diagnosis of early hepatocellular carcinoma related to hepatitis B virus. Omics J Integr Biol. 2020;24:415–23.
22. Wang S, Summers RM. Machine learning and radiology. Med Image Anal. 2012;16:933–51.
23. Teng X, Han K, Jin W, Ma L, Wei L, Min D, et al. Development and validation of an early diagnosis model for bone metastasis in non-small cell lung cancer based on serological characteristics of the bone metastasis mechanism. eClinicalMedicine. 2024;72:102617.
24. Ahn JC, Connell A, Simonetto DA, Hughes C, Shah VH. Application of artificial intelligence for the diagnosis and treatment of liver diseases. Hepatol Baltim. Hepatol Baltim Md. 2021;73:2546–63.
25. Rui F, Yeo YH, Xu L, Zheng Q, Xu X, Ni W, et al. Development of a machine learning-based model to predict hepatic inflammation in chronic hepatitis B patients with concurrent hepatic steatosis: A cohort study. eClinicalMedicine. 2024;68:102419.
26. Kamiyama T, Yokoo H, Furukawa JI, Kurogochi M, Togashi T, Miura N, et al. Identification of novel serum biomarkers of hepatocellular carcinoma using glycomic analysis. Hepatology. 2013;57:2314–25.
27. Chen KL, Gao J. Factors influencing the short-term and long-term survival of hepatocellular carcinoma patients with portal vein tumor thrombosis who underwent chemoembolization. World J Gastroenterol. 2021;27:1330–40.
28. Nan Y, Garay OU, Lu X, Zhang Y, Xie L, Niu Z, et al. Early-stage hepatocellular carcinoma screening in patients with chronic hepatitis B in China: A cost–effectiveness analysis. J Comp Eff Res. 2024;13:e230146.
29. Giuffrè M, Zuliani E, Visintin A, Tarchi P, Martingano P, Pizzolato R, et al. Predictors of Hepatocellular Carcinoma Early Recurrence in Patients Treated with Surgical Resection or Ablation Treatment: A Single-Center Experience. Diagnostics. 2022;12:2517.
30. Llovet JM, Kelley RK, Villanueva A, Singal AG, Pikarsky E, Roayaie S. Hepatocellular carcinoma. Nat Rev Dis Primers. 2021;7:6.
31. Qu C, Wang Y, Wang P, Chen K, Wang M, Zeng H, et al. Detection of early-stage hepatocellular carcinoma in

asymptomatic HBsAg-seropositive individuals by liquid biopsy. Proc Natl Acad Sci. 2019;116:6308–12.
32. Huang A, Guo DZ, Zhang X, Sun Y, Zhang SY, Zhang X, et al. Serial circulating tumor DNA profiling predicts tumor recurrence after liver transplantation for liver cancer. Hepatol Int. 2024;18:254–64.
33. Zhang S, Liu Y, Chen J, Shu H, Shen S, Li Y, et al. Autoantibody signature in hepatocellular carcinoma using seromics. J Hematol OncolJ Hematol Oncol. 2020;13:85.
34. Shaheen KYA, Abdel-Mageed AI, Safwat E, AlBreedy AM. The value of serum midkine level in diagnosis of hepatocellular carcinoma. Int J Hepatol. 2015;2015:146389.
35. Butaye E, Somers N, Grossar L, Pauwels N, Lefere S, Devisscher L, et al. Systematic review: glycomics as diagnostic markers for hepatocellular carcinoma. Aliment Pharmacol Ther. 2024;59:23–38.
36. Hanna-Sawires RG, Schiphuis JH, Wuhrer M, Vasen HFA, van Leerdam ME, Bonsing BA, et al. Clinical perspective on proteomic and glycomic biomarkers for diagnosis, prognosis, and prediction of pancreatic cancer. Int J Mol Sci. 2021;22:2655.
37. Pan Y, Zhang L, Zhang R, Han J, Qin W, Gu Y, et al. Screening and diagnosis of colorectal cancer and advanced adenoma by Bionic Glycome method and machine learning. Am J Cancer Res. 2021;11:3002–20.
38. Blomme B, Van Steenkiste C, Callewaert N, Van Vlierberghe H. Alteration of protein glycosylation in liver diseases. J Hepatol. 2009;50:592–603.
39. Wang L, Liu Y, Gu Q, Zhang C, Xu L, Wang L, et al. Serum N-Glycan markers for diagnosing significant liver fibrosis and cirrhosis in chronic hepatitis B patients with normal alanine aminotransferase levels. Engineering. 2023;26:151–8.
40. Fang M, Zhao Y, Zhou F, Lu L, Qi P, Wang H, et al. *N* -glycan based models improve diagnostic efficacies in hepatitis B virus-related hepatocellular carcinoma. Int J Cancer. 2010;127:148–59.
41. Gui HL, Gao CF, Wang H, Liu XE, Xie Q, Dewaele S, et al. Altered serum N-glycomics in chronic hepatitis B patients. Liver Int. 2010;30:259–67.
42. Rasheduzzaman M, Kulasinghe A, Dolcetti R, Kenny L, Johnson NW, Kolarich D, et al. Protein glycosylation in head and neck cancers: From diagnosis to treatment. Biochim Biophys Acta BBA - Rev Cancer. 2020;1874:188422.
43. Peixoto A, Relvas-Santos M, Azevedo R, Santos LL, Ferreira JA. Protein glycosylation and tumor microenvironment alterations driving cancer hallmarks. Front Oncol [Internet]. 2019;9:380.
44. Nie H, Liu X, Zhang Y, Li T, Zhan C, Huo W, et al. Specific N-glycans of hepatocellular carcinoma cell surface and the abnormal increase of core-α-1, 6-fucosylated triantennary glycan via N-acetylglucosaminyltransferases-IVa regulation. Sci Rep. 2015;5:16007.
45. Cui J, Huang W, Wu B, Jin J, Jing L, Shi WP, et al. N-glycosylation by N-acetylglucosaminyltransferase V enhances the interaction of CD147/basigin with integrin β1 and promotes HCC metastasis. J Pathol. 2018;245:41–52.
46. Wang Y, Chen H. Protein glycosylation alterations in hepatocellular carcinoma: Function and clinical implications. Oncogene. 2023;42:1970–9.
47. Ferreira JA, Magalhães A, Gomes J, Peixoto A, Gaiteiro C, Fernandes E, et al. Protein glycosylation in gastric and colorectal cancers: Toward cancer detection and targeted therapeutics. Cancer Lett. 2017;387:32–45.
48. Thomas D, Rathinavel AK, Radhakrishnan P. Altered glycosylation in cancer: A promising target for biomarkers and therapeutics. Biochim Biophys Acta BBA - Rev Cancer. 2021;1875:188464.

How to cite this article: Su R, Tao X, Yan L, Liu Y, Chen CC, Li P, et al. Early screening, diagnosis and recurrence monitoring of hepatocellular carcinoma in chronic hepatitis B patients based on serum N-glycomics analysis: A cohort study. Hepatology. 2026;83:40–56. https://doi.org/10.1097/HEP.0000000000001316